Influence of Variations in a Mechanical Framing Station on the Shape Accuracy of S-rail Assemblies

Klaus Wiegand[1], Tobias Konrad[1], Marion Merklein[2]

[1] Daimler AG, Sindelfingen, Germany
[2]Institute of Manufacturing Technology, Erlangen, Germany

1 Abstract

In virtual production planning, recent publications have shown the possibility of creating a digital process chain of body parts including the process steps in the press shop and body-in-white shop. The digital process chain is used to get an early impression of the dimensional accuracy of assemblies regarding the single parts that are used. Within the entire process chain, a wide variety of factors influence the dimensional accuracy of (sub)-assemblies. However, not every parameter of the deep drawing and assembly process exerts significant influence on the assembly quality and on process stability. Furthermore, the interaction of certain parameters could lead to an improved result at the end of the process chain.
For this reason, sensitivity and robustness analyzes applying LS-OPT are used to detect factors influencing the shape accuracy of single parts and assemblies. This contribution covers the shape deviation behavior of single parts in the press shop and their state after parameter variations in a virtual framing station. The aluminum alloy AA6014 and the mild steel alloy CR3 with a sheet thickness of 1.0 mm are investigated.
Parameter variations of the clinching process are presented in this paper by joining an S-rail specimen. The S-rail geometry shows a visible und measurable shape deviation behavior.
Finite element tools, such as LS-DYNA and Abaqus, are applied to model an S-rail assembly process. Following a feasibility simulation regarding cracks and wrinkles, the simulation process is used to detect the significance of factors in the digital process chain with respect to the dimensional accuracy of assembled components.
Besides this aspect, the finite element simulation is subsequently used to optimize the assembly process of S-rails in the framing station.

2 Introduction

Nowadays, a clear statement on the shape accuracy of the formed and assembled parts at a very early stage of the product development and development process is important. As part of the dimensional accuracy of formed parts – springback behavior being the deviation to the nominal geometry – crack formation and 1st and 2nd order wrinkling as well as surface defects like stretcher strains are further analyzed as quality criteria [1].
Due to shorter product development cycles, increasing diversity, and an increasing number of variants of outer parts, the use of digital product optimization methods is essential for the dimensional accuracy of both single parts and joined assemblies. According to the „Rule of ten“, introduced by Tilo Pfeifer, the detection of non-tolerable dimensional deviations of assemblies at an earlier stage (Design – Planning – Equipment Manufacture – Production) results in a failure cost advantage factor of 10 per stage [3]. Accordingly, it is necessary on the one hand to use a linked forming and joining process simulation in order to visualize and detect significant influencing factors on the dimensional accuracy of single and assembled parts both in the press shop and the body shop process steps. On the other hand, the sensitivity analysis should be employed for choosing and filtering important and quantifiable factors with respect to less-important influencing factors on the shape accuracy of single parts in the press shop. Furthermore, suitable influencing factors of the sensitivity analysis are input factors for the next step – a combination of robustness analysis and optimization.
Subsequently, the results of the sensitivity analysis can first be used to obtain derived measures for an enhancement or a reduction of the wide range of control parameters. In addition, by varying several control parameters and the standard deviation from non-measurable disturbance variables, the sensitivity analysis is useful for gaining in-depth process knowledge.
Based on the sensitivity analysis, the robustness analysis is the next analytical step of the various process chain steps for the specimen used. The aim of the robustness analysis herein is to find out to what extent the non-predictable and determinable variations and the defined noise variables are responsible for effects on the dimensional accuracy of the S-rail specimen.

Using the optimization tool LS-OPT, as a first step possible control parameters in the forming simulation are investigated and analyzed with regard to their overall impact on the springback behavior and the nodes displacement of the specimen. Regarding both the stress results and the shape deviations of a robust parameter combination, these preliminary tests are required for coupled investigations of several station parameters of a mechanical framing station. The aim is on the one hand to identify relevant influencing factors for single parts and hence for the dimensional accuracy of assembled parts, and on the other hand to transfer the methodical approach – consisting of a coupled sensitivity and robustness analysis - to the joining process chain. Suitable variation possibilities of parameters in the virtual mechanical framing station are pointed out.

3 Sensitivity and robustness analysis in the press shop

A definition of the terms sensitivity and robustness defined control and noise parameters is required before analyzing the specimen S-rail in terms of its sensitivity and robustness attributes. Afterwards, the current relevance of this issue is presented discussing former papers on investigated forming process chains. In conclusion, the approach of transferring and coupling used for simulative und optimizing methods in the forming process to the joining process is presented as an additional topic.

3.1 Terms of sensitivity and robustness analyses

Literature research yielded a huge variety of miscellaneous definitions for the terms sensitivity and robustness in a virtual context.
The sensitivity analysis represents the initial step of a coupled and a consecutive sensitivity and robustness analysis. According to formula 1, Grossenbacher [4] referred to sensitivity SEN as a gradual, quantitative change of the output variable, caused by a modification of the input variable.

$$SEN = \frac{\Delta x}{\Delta y} = \frac{\Delta Output}{\Delta Input} \tag{1}$$

Regarding sensitivity analysis, there is a distinction between local (single design-points) and global (whole design space) coefficients of sensitivity [5]. Further on, these coefficients of sensitivity can be calculated based on linear regression methods or on the basis of a, variance-based approach [6]. For the purpose of this work, the sensitivity analysis takes into account the entire parameter of space and its interactions, with a specification of the control parameters' range. Furthermore, a probabilistic concept is followed up for the constituting interactions between the individual influencing factors. Target figures include both single and aggregate effects of the input parameters (including summation of the interactions) on the springback behavior in the x-, y- and z-directions as multiple output variables.
For evaluating the dimensional and shape accuracy of single and assembled parts, the effect of variations of the noise variables is interesting, followed by the identification und elimination of non-significant input variables of the sensitivity analysis. Processes are robust and, according to Kleppmann, insensitive to process influences, if the influence of non-predictable variations of noise variables is as low as possible [7]. The approach taken by this contribution is to use the robustness analysis in order to make a statement about the robustness-optimized design points of the sensitivity analysis. Finally, the specimen used for this contribution is supposed to highlight the robust design optimization of a forming and joining process chain.

3.2 Enhancement of sensitivity and robustness analyses to the assembly process

Recent parametric studies investigated the sensitivities, e.g. of the blankholder force or the friction coefficient on an output variable like the springback behavior used without performing a robust design optimization [8]. In contrast, there are multiple publications dealing with the sensitivity and robustness analysis of both real and simulated forming processes using sheet metal parts. As one of the results thereof, the influence factors were categorized and used for the authors' investigations. Suitable groups were established: influencing factors of the forming process used, presses, tools [9], as well as the material properties and specimen sizes and their positions on the die [10]. For this reason, parameter identification of relevant influencing factors is not the main focus for this investigation. Therefore, some relevant process parameters obtained from previous pilot tests are selected for explaining the methodical approach.
Although the literature yields other investigations with a flex-rail tool [11] that showed a coupled virtual forming and joining process chain, the article mentioned did not focus on sensitivity and robustness analyses relevant influencing factors during the various successive forming and joining process steps. Additionally, the dimensional accuracy or the springback behavior was judged in the form of an

example by using a punctiform thermal joining process. Accordingly, the idea here is to perform a coupled sensitivity and robust optimization using the selected S-rail specimen. The objective is to present the possibility of investigating and analyzing relevant influencing factors of assembled parts as a supplement to a coupled forming and joining process chain.

4 Sensitivity analysis of the process chain of the S-rail specimen

Based on the benefits of using the S-rail specimen for investigating the influencing factors during the forming and joining process chain, this chapter shows the simulation setup of the forming process. Secondly, the methods and approaches used for visualizing and calculating the sensitivity and robustness analysis of the forming process S-rail are presented. This chapter concludes with the evaluation of the results generated.
Thanks to existing preliminary investigations and validations of the S-rail forming simulation using FE-CODE LS-DYNA, it is possible to make statements about the sensitivities of various input variables on the springback behavior. Moreover, first pilot tests conducted reveal a quantitatively high and controllable springback behavior of the geometry through an adaptive blankholder force. Moreover, the S-rail specimen geometry combines both convex and concave shapes within a single part, hence allowing for suitable conclusions as to the influence of the geometry's shape on the dimensional accuracy of assembled parts.

4.1 Setup sensitivity and robustness analysis of the process steps in the press shop

On the one hand, Fig. 1 points out the four different basic solver calls (Gravity-Hold-Drawing-Springback) and additional steps like cutting/flanging of the S-rail forming process chain. On the other hand, Fig.1 illustrates the investigated geometries with a parallelogram-shape and a S-shape, using an initial size of 224 x 294 mm.

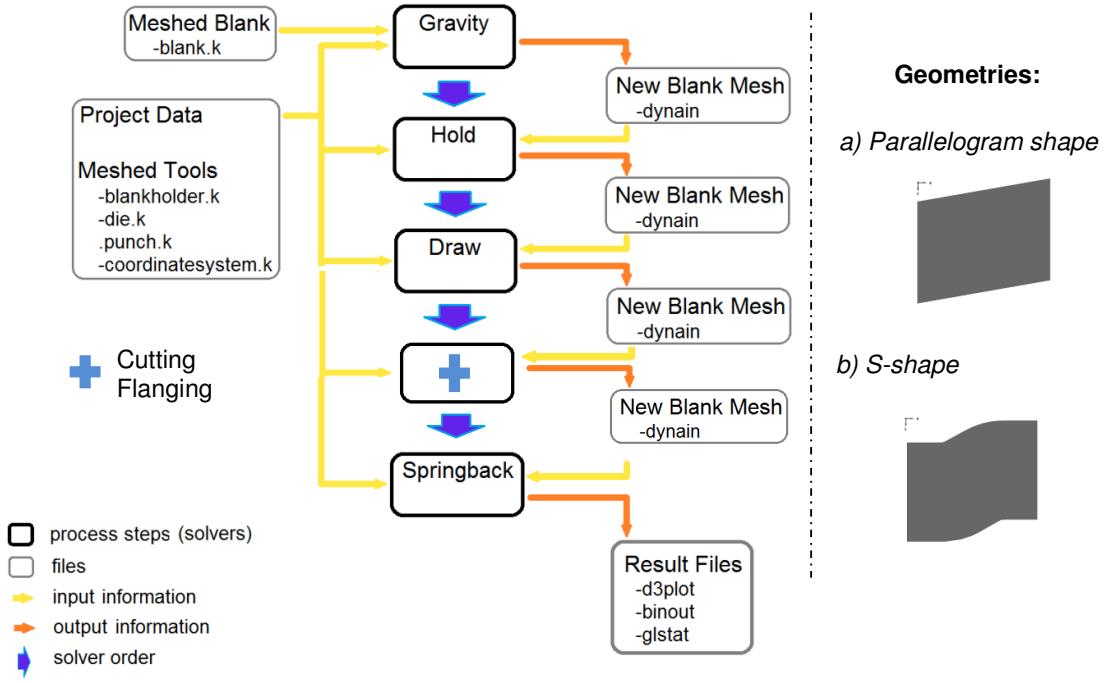

Fig.1: Setup simulation of the S-rail deep drawing process with LS-DYNA

Preliminary deep-drawing tests of geometry b (see Fig.1) show lower springback values compared to the geometry variant a. The S-rail specimen is simulated using a draw depth of 40 mm and an initial blank-holder force of 90 kN. In this contribution the FE code LS-DYNA Version 971 Revision 7.1.1 developed by LSTC is used.
The aluminum alloy AA6014 and the mild steel alloy CR3 with a sheet thickness of 1.0 mm are used as material for the sensitivity and robustness analysis. Table 1 displays both an excerpt of the basic material parameters and properties and the elastic-plastic material behavior applying the Barlat YLD2000 yield criterion [12].

Material	δ_0 MPa	E MPa	A %	α_1	α_2	α_3	α_4	α_5	α_6	α_7	α_8	M
AA6014	132	68000	6	1.05	0.95	1.01	1.01	1.00	1.06	0.96	1.01	6
CR3	164	204000	4	1.26	1.03	0.87	0.99	0.98	1.07	1.08	0.99	4

Table 1: Material properties and yield locus Barlat YLD2000 of AA6014 and CR3 (s = 1.0 mm)

As stated in first preliminary investigations, appropriate control and noise parameters were determined for the sensitivity and robustness analysis. Using LS-OPT Version 5.1.1 suitable sensitivity and optimization methods are set for both the sensitivity and robustness analysis.
According to Fig. 2, the sensitivity analysis with the steps visualized below is the first step prior to performing a Robust Design Optimization (RBDO). The control parameters of the sensitivity analysis are selected from 55 possible input parameters in the LS-DYNA project data file: blankholder force (60-120 kN), x-y translation of the plate's position (-10 to 10 mm) and sheet thickness (0.95-1.05 mm).

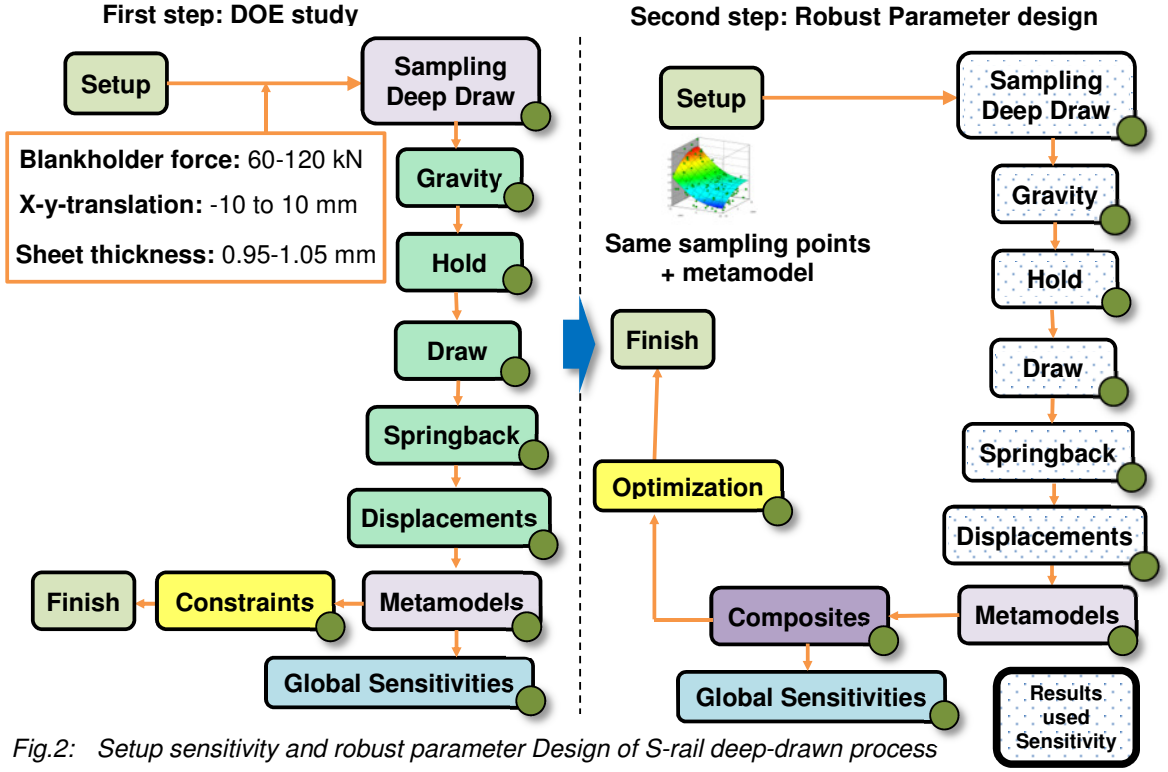

Fig.2: Setup sensitivity and robust parameter Design of S-rail deep-drawn process

Altogether, 200 simulation points are performed and the appropriate solver calls made for the DOE study. As a sampling method, the Latin Hypercube method is preferred over the sampling method for reasons of time advantage and a somewhat better distribution of the design points. Furthermore, one approach among others was to revert to the metamodel Radial Basis Function Network [15]. Due to the high calculating accuracy, speed and flexibility with respect to the interpretation of the sensitivities of the springback behavior, this regression-based metamodel is appropriate for the given application, with a local refinement of both sampling points and with elimination of the numerical noise/scatter [13]. 200 sampling points as well as a generic optimization algorithm with a population size of 50 and the number of 50 generations are chosen for the robustness analysis. By using a multi-objective mode, a Pareto-optimal frontier is generated. In analogy to the sensitivity analysis, Latin Hypercube is selected for the point selection method and the radial basis function network for the metamodel. Furthermore the results of the first step sensitivity analysis are used for filtering non-significant influencing factors for the robustness analysis.
For both the sensitivity and the robustness analysis, it is necessary to define responses correspondent to Table 2. The aim is to minimize these responses by using the shown approach of robust design optimization. Mean values and standard deviations of the nodes' displacement in x-, y- and z- direction as well as the resulting vector are set and analyzed for the sensitivity analysis.

Response	Used for Optimization	Abbreviation	Explanation
Mean values	X	MEAN_*(direction)*	Mean value of all displacements of the specific coordinate direction
Standard deviations	X	STD_*(direction)*	Standard deviation of all displacements of the specific coordinate direction
Mean values x standard deviations	+ (objective)	OBJ_*(direction)*	Standardized mean value as a product of mean value and standard deviation
Thickness reduction	+ (constraint)	THICK_RED	Definition of the maximum thickness reductions at the individual nodes
Distance to FLC	+ (constraint)	FLD_DIST	Definition of a lower percentage distance to the Forming Limit Curve

Table 2: Response for the sensitivity and objectives/constraints for the robustness analysis

Regarding the sensitivity analysis, the influence of the control parameters on the mean values, standard deviations and coupled terms on the nodes' displacements are valuated as an indicator for the springback behavior.

4.2 Results of the sensitivity and robustness analysis

Different qualitative evaluation methods are used for evaluating the influence and sensitivity of various influencing factors on nodal displacement (OBJ_X, OBJ_Y and OBJ_Z). Besides linear correlations bars, global sensitivities plots are discussed and compared to each other. Linear correlation bars show the effect of the input variables on one output variable. In addition, Fig. 3 shows standardized values of the global sensitivity analysis. According to Fig. 3, the y-translation of the plate in reference to the initial insertion position has the greatest influence on the three objective responses.

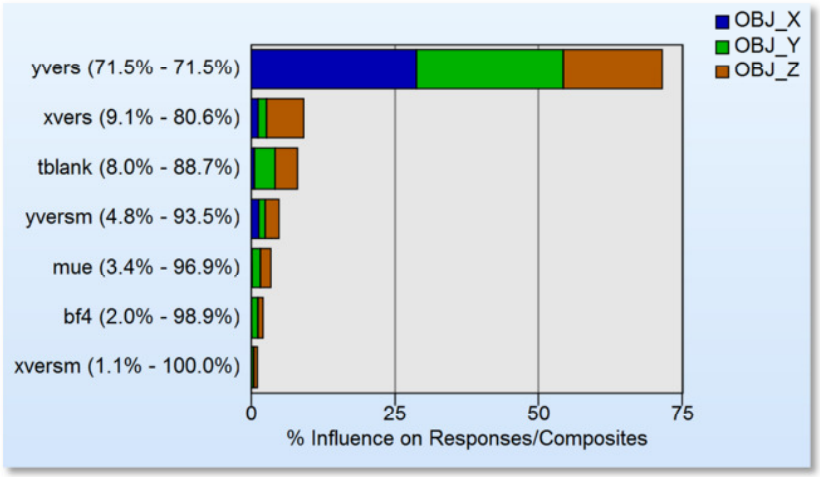

Abbreviation	Explanation
yvers	y-translation
xvers	x-translation
tblank	Thickness
mue	Friction coefficient
bf4	Blank holder force

Iterations: 200
Sampling: Latin Hypercube
Metamodel: Radial Basis Function Network
Geometry: S-shape

Fig.3: Global sensitivities of the selected influencing factors on the springback behavior

On the one hand, Fig. 3 qualitatively visualizes the influences of each parameter as both singular and cumulated values, sorted by the relevance of each influence on the responses. In accordance with Fig. 3, however, 89 % of the influence on the nodal displacements in three coordinate directions can be explained by varying three of the six registered control and noise parameters. Furthermore, the correlation matrix is used for a detailed itemization of the impacts on the response dimensions and for detecting positive and negative interactions with each other. After considering the correlation matrix, all defined control parameters exhibit only small positive or negative correlations in the -0.06 and 0.13 ranges and as a consequence are considered as independent input variables.
In parallel, metamodels are considered for all defined responses in Table 1. As an example, according to Fig. 3, a metamodel including the greatest influencing factors (x-, y-translation of the plate) and the response function OBJ_Z is visualized in Fig. 5. Furthermore, it is essential to examine the accuracy of the metamodel's approximation predicted by calculated values - by using the visualized quality criteria. The illustrated metamodel points out the tendency of an influence of the x- and y-displacement of the original blank position on the OBJ_Z response. A look at Fig. 4 visualizes that the shown response surface displayed evinces non-linear relations between input and output variables.

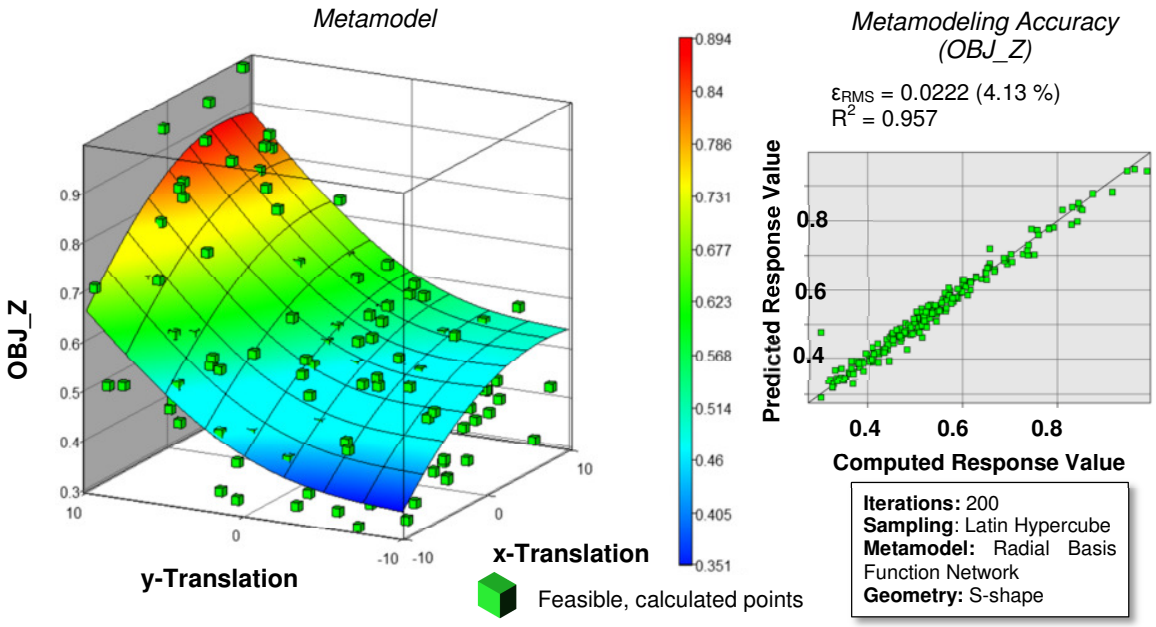

Fig.4: Metamodel (left) and its accuracy for the objective weighted mean value of z-displacement

An error analysis of the established metamodel gives evidence of a good match of the predicted and computed response values. For an assessment of the metamodel's quality, a look at the root mean square error ε_{RMS} (RMS) – as the difference between the predicted and the computed response values – shows a maximum failure of 4.13 %. In addition, the coefficient of determination R^2 proved that 96 % of the data variation can be explained by the metamodel. As a result, the metamodel is used for analyzing the process robustness based on predicted values.

In conclusion, the result of the sensitivity analysis suggests the filtering of the most important parameters for the robustness analysis: yvers, xvers, bf4 as control parameters and tblank and mue as noise variables. Due to the high coefficients of determination and low error values, all metamodels of the responses (Table 2) can be used for the investigation of the robustness. On this basis, computation time for the robustness analysis can be saved.

For analyzing the resulting sigma level of each objective, three composites are introduced. The selected noise variables of the robustness analysis are normally distributed fluctuating with Six-Sigma-levels of six standard deviations around its mean values. Several optimal design points were computed iteratively using in total seven control and noise variables. As an instance of an optimal design point for the objective OBJ_Z an x- and y-translation of -9.5 mm was calculated.

The multi-objective optimization led to a three-dimensional, optimal Pareto front of the shown robustness objectives in Fig. 5. The trade-off plot below exposes the three desired objectives of this robust design parameter optimization.

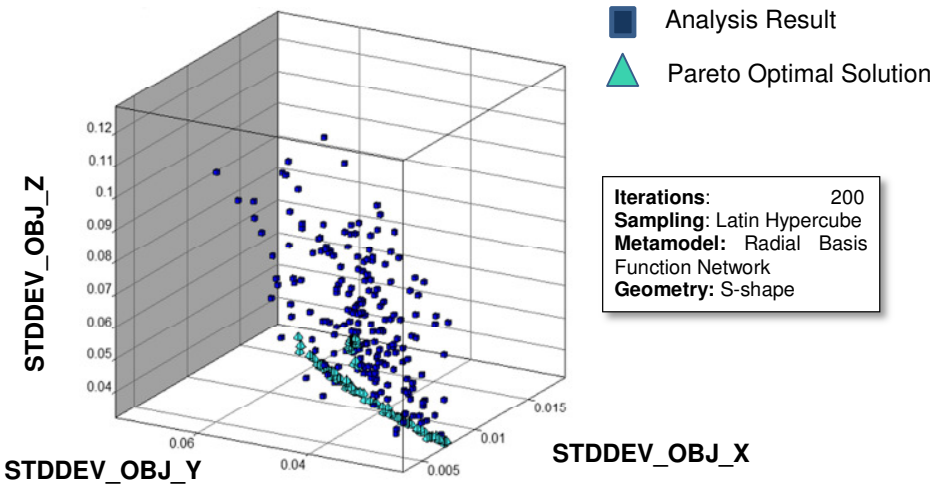

Fig.5: Trade-off plot of the standard deviations of the objectives x-z

According to a high confidence interval a large certainty for predicted values, the standard deviation of each objective STDDEV_OBJ_*X(Y/Z)* correlating with the sigma level is investigated and minimized.
The Pareto optimization of Fig. 5 show both the analysis results (blue cubes) and Pareto optimal solutions (green pyramids). The evaluation of this trade-off plot is based on three equal weighted objectives. The green pyramids visualize solutions for which a minimization of all three objectives is the aim. Compared to the analysis results with standard deviations of a 0.12 mm springback behavior in z-direction, the Pareto optimal solutions reduced it to one third. Further investigations take the comparison of calculated and predicted response distributions into account.

4.3 Evaluation sensitivity and robustness analysis

Linking the sensitivity and robustness analysis demonstrated a method for filtering non-significant input parameters and using generated metamodels for the whole process chain. In addition, the investigations are possible for various types of materials/material properties. Reliable results are possible due to low failure predicting rates of the metamodels. In terms of the feasibility simulation regarding cracks, thinning and wrinkles, the parameter sets did not show any quality defects.
In conclusion, it is possible to transfer optimized parameter sets and the corresponding result quantities to the joining process chain. Furthermore, a statement regarding the influence of the accuracy of single varied parts on the dimensional accuracy of assembled parts could be given.

5 Linked forming- and joining process chain of the S-rail specimen

Preliminary tests showed that not every significant influencing factor for the forming process chain exerts significant influence on the dimensional accuracy of assembled parts. Joining operations like clinching processes are influenced by other process and material parameter sets. Furthermore, regarding the entire process chain, interactions between influencing factors of the forming and the joining process have a superposed effect on the dimensional accuracy of the assemblies. Therefore, it is essential to transfer both the shape deviations compared to the CAD data files and result quantities to the joining process chain.

5.1 Methodology

In order to demonstrate and analyze the influence of relevant factors of the single forming and joining steps on the shape accuracy of assembled parts, a specimen is useful for understanding its parameter coherences and dependencies. The research focuses on the influencing factors of a virtual mechanical framing station depending on the used material. For this purpose, parametric studies with a variation of influencing factors of a mechanical framing station are performed. Divided in two investigated steps, first of all the nominal CAD geometry is used for the variation of the joining boundary conditions. As a second step, the impact of the forming simulation on the dimensional accuracy is used for analyzing the influence of the deep drawing simulation. For that, different mapping and morphing methods are applied. Fig. 6 visualizes the principal scheme for both a linked deep drawing and mechanical clinching process chain and the setup with the used shapes.

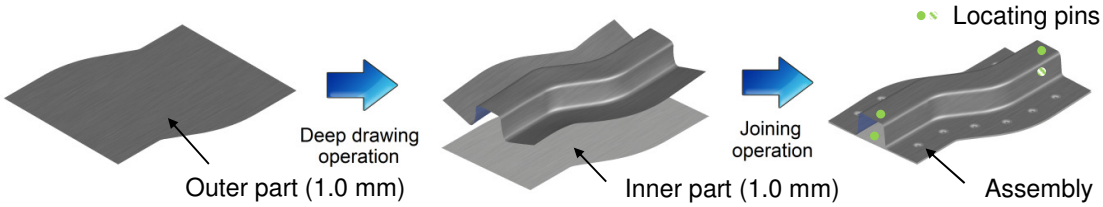

Fig.6: Connection of the simulative S-rail deep drawing and joining chain

The developed methodology provides the necessary structure and process workflows to extend it to other geometrical shapes and material properties. Supplementary, both the number of sheet metal forming steps and the number of joining steps can be varied. Furthermore, it is possible to change the number of single components of outer and inner parts.

5.2 Application of mapping methods

In this approach, mapping methods are used to transfer results from an optimized and robust (regarding selected influencing factors) LS-DYNA FE code of the forming simulation to the Abaqus input deck of the joining simulation. For the transformation of nodal and element result quantities of the outer part both the SIMAN Mapper from INPRO and the SCAI Mapper from the Fraunhofer Institute are considered. The objective is to transfer data between the different source mesh (LS-

DYNA output mesh) and the target mesh (Abaqus input mesh). Due to the adaptivity in uniform remeshing using LS-DYNA and the initial element size of 8 mm, the source mesh has an irregular mesh density after the forming process. Furthermore, the source mesh exhibits a combination of quads and triangles as element formulations. The required mesh quality of individual outer part regions for the calculation of the joining simulation differs, especially in the flange zones, from the forming simulation. Due to this fact, the original CAD geometry according to specifications based on add-on parts, like doors, hoods and trunk lids, is meshed using common meshing tools like HyperMesh or ANSA.
Fig. 7 visualizes the results of mapping operations performed with the software components used – excluding the previous both manual and automatic positioning steps of the source mesh to the target mesh.

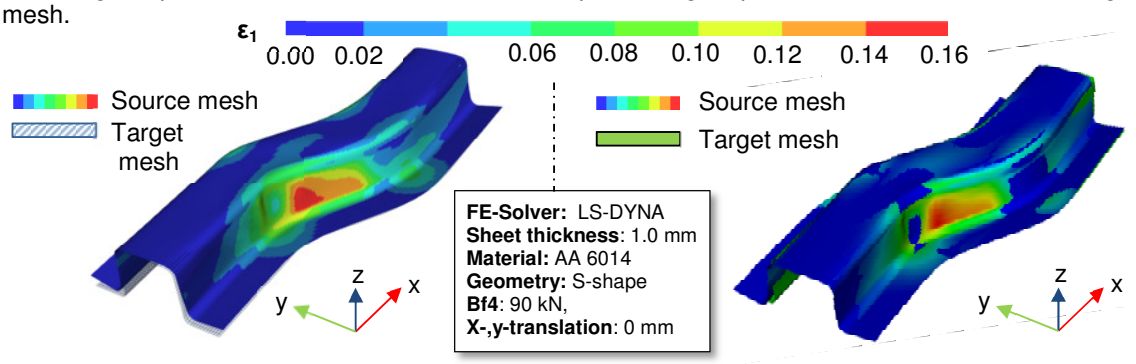

Fig.7: Mapping method of the element strain ε_1 of the outer part – LS-DYNA (source mesh) to Abaqus (target mesh) using the SIMAN-Mapper (left) and the SCAI-Mapper (right)

According to an initial feasibility study, due to the S-shaped plate geometry, S-rail forming simulations showed the dimensional deviation in x-direction compared to CAD data visualized in Fig. 4. This dimensional deviation can be seen in Fig. 4 above by the application of the mapping tools mentioned. Both transfer of (plastic) strains and a mapping of the part outline have been achieved successfully. Small deviations of the mapping process of the target from the source material properties based on different mesh qualities.
Moreover, incremental morphing methods to transfer the shape deviation of the formed parts to the next step in the process chain are investigated. By doing so, missing points are interpolated.

5.3 From a single S-rail to the S-rail assembly

In addition to the target mesh of inner and outer part, further specifications are required to perform the joining simulation operation. The clinching process is performed at the two outer flanges of the specimen investigated. Either an uncut, formed outer part based on the S-shape plate or the preferred cut part with a continuous flange length of 30 mm can be used. A minimal flange length of 18 mm is limited on nominal outer diameter of 8 mm. In addition, the minimum spacing of the joints' center of the part of 7 mm and the minimum applicable spacing between two joints of 20 mm is taken into consideration. According to the insertion consequence of Fig. 6, first the laser-cut inner part of a sheet thickness of 1.0 mm and two locating pins is loaded. Afterwards, the formed outer part is loaded and provides two centering pins by analogy to the inner part. These centering pins are used both for the measurement recording and the positioning in the virtual mechanical framing station according to the 3-2-1 mess principle. Joining and clamping conditions are part of the variations in a mechanical framing station of an S-rail assembly.

6 Variations in a virtual mechanical framing station of an S-rail assembly

In this chapter, several variation possibilities in a mechanical framing station of an S-rail assembly process are shown. Especially variable boundary conditions in a virtual mechanical framing station are investigated and varied as a compulsory investigation of existing publications [14]. The clinching process of an S-rail assembly process means is chosen as an example. Finally, an excerpt of the results of the variation possibilities of the boundary joining conditions is demonstrated.

6.1 Investigated and varied factors of a virtual mechanical framing station

An extract of possible boundary conditions a virtual mechanical framing station is shown in Fig. 8.

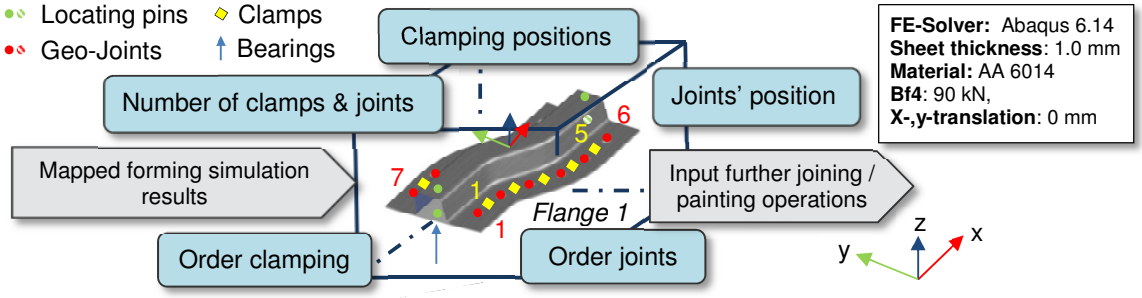

Fig.8: Investigated parameters in a virtual mechanical framing station

At the beginning, the number and position of the six joints of a diameter of 8 mm are distributed equally on each flange side in consideration of the minimal distance between two joints. The initial number of five clamps on each flange side is defined to investigate the influence of clamping conditions between two joints on the dimensional accuracy of the assembled parts. Similar to Fig. 8, the numeration both of the joints and the clamps begins at the lower end of the flanges (negative x- and y-direction). The joints' position is designed that the y-distance of the joints' centers to the flange edge and the discharge radius is the same.
Additionally, the order of clamping and joints is interesting to consider. Depending on the joining sequence, the inner and outer part can be initially joined "from the outside to the inside" (sequence#1 - flange1: 1-6-2-4-3) or "from the inside to the outside" (sequence#2 - flange1: 3-4-2-5-6-1). In analogy to the joints, the clamping process starts in an adjacent region of the joint. An extended investigation will deal with the consideration of the number of clamps and joints depending on the material used.

6.2 Settings and results of the initial joining simulation of an S-rail assembly process

The investigations of the influence of the mechanical framing station parameters starts by using the nominal CAD geometry data of the outer and inner parts. The joining and the clamping sequence are determined according to sequence#1. An existing substitute model is utilized for the clinching process. Therefore, a rigidity value of the coupling is set in analogy to previous investigations. As a response, both the resulting von Mises stress and the reuslting strain values are considered. Fig. 9 shows the principal strain components at the integration points and the von Mises equivalent tensile stress after performing the steps gravity, clamping, joining and an orientated measurement step.
Fig. 9 visualizes the influence of the joints and clamps on the strain and stress components of the adjacent elements. As an example, regarding the influence of a joint (Pos.1) and a clamp (Pos. 2) shows a qualitative greater influence of the joint on the selected stress and strain components of the neighbor elements.
Furthermore, Fig. 9 evinces by tendency higher stress and strain values at the radius at Pos.3. Beneath the interaction between clamping and joining positions, the convex-concave S-Rail geometry seems to have an influence on the result quantities. Because of that, a parametric study of various joining and clamping conditions is performed regarding the influence of the nominal CAD geometry.

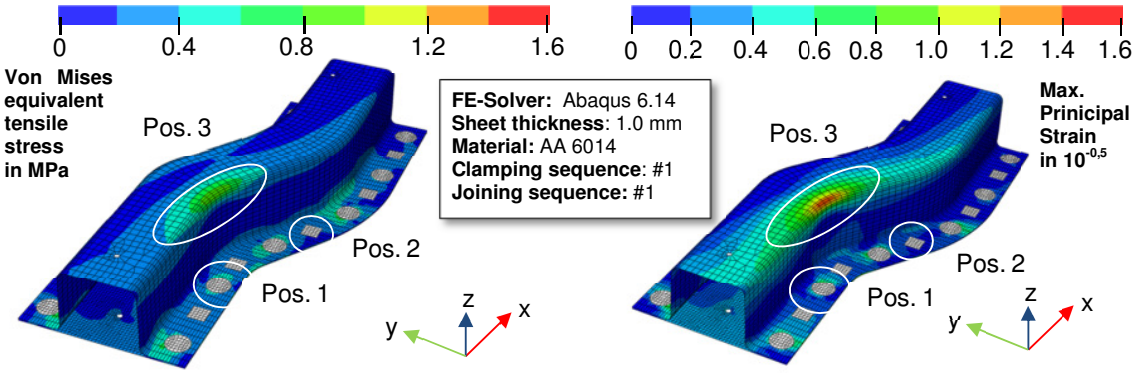

Fig.9: Von Mises equivalent tensile stress (left) and max. principal strain components (right) after the S-rail joining process

Additionally, regarding outer parts with a non-dimensional accuracy based on the forming process, the displacements in z-direction after the joining process is compared to its deep-drawn formed state. Due to the aim of the evaluation of the influence of the defined framing station parameters, parallel measurements und considerations of the responses are necessary both before starting and after finishing the joining process.

7 Summary and Outlook

As a summary of this contribution, it can be said that this S-rail assembling process is a further example for the linking of several variations of forming and mechanical joining simulations. The application of various mapping tools serves the transfer of simulation results, such as stress quantities, from the LS-DYNA FE code to other codes, such as Abaqus.
Furthermore, the evaluation of the sensitivity analysis of the S-rail forming process points out that the x-translation of the plate has a higher influence on the dimensional accuracy compared to the y-translation. Compared to these parameters, a variation of the blankholder force seems to not have a significant influence on the dimensional accuracy. According to the response variables selected, the evaluation methodology is used to get an impression of the influence of control and noise variables on the mean values, standard deviations and coupled, weighted terms of the nodes' displacement. Due to a determined high accuracy of the metamodels of the sensitivity analysis, the calculation time is reduced as the results of 200 iterations of the forming steps can be used for the robustness analysis. Subsequent to the assumptions of a linked sensitivity- and robustness analysis of the forming process, S-rail experiments are performed to validate the results.
Beneath various parameter sets of the forming simulation, variation possibilities in a virtual mechanical forming station are presented and partially investigated. In this connection, this influencing analysis method of the forming simulation can be used for both a single and a linked consideration of the influencing factors of a mechanical framing on the shape accuracy.

8 Literature

[1] Kästle, C.; Liewald, M.; Roll, K.: "Springback Simulation of the Process chain Press Line Forming and Roller Hemming Processes", In: 9. Key Engineering Materials Vol. 549, Trans Tech Publications, 2013, S. 231-238

[2] Wiegand, K., Zubeil, M., Roll, K.: "Einsatz der Simulation in der Prozesskette Karosseriebau. LS-DYNA Forum" – Keynote Vortrag, Bamberg 2010, p. 53-59

[3] Pfeifer, T: "Zusammenhang zwischen Phasen der Fehlerverursachung und den Fehlerkosten", Quality management, 1996

[4] Grossenbacher, K.: "Virtuelle Planung der Prozessrobustheit in der Blechumformung", Dissertation, ETH Zürich, 2008

[5] Fleischhauer, R.: "Lineare und nichtlineare Sensitivitätsmaße bei der Strukturanalyse, Großer Beleg, Institut für Statik und Dynamik der Tragwerke", Universität Dresden, 2009

[6] Han, S.-O.: Varianzbasierte Sensitivitätsanalyse als Beitrag zur Bewertung der Zuverlässigkeit adaptronischer Struktursysteme, Dissertation, TU Darmstadt, 2011

[7] Kleppmann, W.: „Taschenbuch Versuchsplanung", Hanser, München, Wien, 2008

[8] Papeleux, L., Ponthot, J.P., 2002: "Finite element simulation of springback in sheet metal forming, Journal of Materials Processing Technology 125–126, 785–791.

[9] Hein, P., Mercuzot, G., Devin, J.-M., Fouques, D.: "Methology for Springback control in stamping of AHSS", SCT 2008, Future trends in steel development, processing technologies and applications, Wiesbaden, 2008

[10] Whang, Z.: "Design for uncertaincies of sheet metal forming process", Dissertation, Ohio State University, 2007

[11] Govik, A.; Nillson, L.; Moshfegh, R.: "Finite element simulation of the manufacturing process chain of a sheet metal assembly", Journal of Materials Processing Technology 212 (2012) 1453-1462, Sweden, 2012

[12] Barlat, F., Brem, J.C., Yoon, J.W., Chung, K., Dick, R.E., Lege, D.J., Pourboghrat, F., Choi, S.H., Chu, E., 2003: Plane stress yield function for aluminum alloy sheets – part 1: Theory. International Journal of Plasticity 19, 1297–1319.

[13] Bishop, C.M.: "Neural Networks for Pattern Recognition", Department of Computer Science and Applied Mathematics, Oxford, 1996

[14] Eckert, A.: "Prognose der Maßhaltigkeit punktförmig mechanisch gefügter Karosseriebauteile", Dissertation, Fraunhofer-Institut für Werkzeugmaschinen und Umformtechnik, Chemnitz, 2012

[15] Orr, M.: „Introduction to Radial Basis Function Networks", Centre of Cognitive Science, Edinburgh, 1996